Indian Journal of Traditional Knowledge
Vol 19(2), April 2020, pp 350-359

# Analysis of RIG-I-mediated innate immune response in rats with Kidney-Yang Deficiency Syndrome and its change following Yougui pill administration

Min Huang[1], Junfeng Liu[2], Min Xiao[1], Xiaoming Yu[1], Yanyan Zhou[1], Aihua Tan[1] & Min Zhao[1,*,+]

[1]School of Basic Medical Sciences, Hubei University of Chinese Medicine, Wuhan, 430 065, China

[2]Key Laboratory of Traditional Chinese Medicine Resource and Compound Prescription, Ministry of Education, Hubei University of Chinese Medicine, Wuhan, 430 065 China

E-mail: [+]zmin13@hbtcm.edu.cn

*Received 26 September 2018; revised 15 January 2020*

Kidney-Yang Deficiency Syndrome (KYDS) is closely bound up with the immune response of immunocompromised patients. The study is to investigate whether retinoic acid-inducible gene-I (RIG-I)-mediated innate immune response participates in the development of KYDS in rats and evaluate the effect of Yougui pill (YGP) on the response in KYDS rats. KYDS rats were induced by intramuscular injection of hydrocortisone at the dose of 10 mg/kg/d for 15 days. YGP at concentrations of 2.43 g/kg/d and 4.86 g/kg/d were administered intragastrically to KYDS rats for 30 days. The results showed that the body weight, urinary 17-hydroxycorticosteroid (17-OHCS) level, spleen size and spleen index in KYDS rats were significantly decreased compared with healthy control rats, while YGP treatment reversed them towards normal level in a dose-dependent manner. Moreover, KYDS challenge not only strikingly increased the mRNA and protein expression levels of RIG-I, tripartite motif containing 25 (TRIM25), tumor necrosis factor-α (TNF-α) and interleukin-6 (IL-6) but also markedly enhanced the endogenous RIG-I polyubiquitination levels. Whereas, YGP treatment effectively reversed this tendency in a dose-dependent manner. In conclusion, these findings revealed that RIG-I-mediated innate immune response was closely bound up with the development of KYDS. And YGP exhibited certain anti-inflammatory effects on KYDS rats via inhibiting the RIG-I-mediated innate immune response.

**Keywords**: Interleukin-6, Kidney-Yang deficiency syndrome, Retinoic acid-inducible gene-I, Tripartite motif containing 25, Tumor necrosis factor-α, Yougui pill

**IPC Code:** Int. Cl.[20]: A61K 31/353, A61K 31/7105, A61K 31/203, C12N 15/117, A61K 38/37, A61J 7/02

Kidney-Yang Deficiency Syndrome (KYDS) is a crucial concept of Traditional Chinese Medicine (TCM). The characteristic symptoms of KYDS patients mainly includes fatigue, thin stool, hearing impairment, soreness and weakness of waist and knees, looseness of teeth and cold feeling of whole body. Recently, with the development of animal experiments, KYDS has attracted the attention of many researchers[1-4]. Based on the fact that the unbalance of adrenal cortex hormones plays an essential role in the pathogenesis of KYDS, hydrocortisone, a kind of steroid hormone produced by adrenal gland cortex, has been used to establish animal models with KYDS. Virtually, hydrocortisone injection is the most popular method to make the model of KYDS[5-7]. Representative signs in the rats treated by hydrocortisone, including fatigue, weakness, reduced activity, weight loss, slowed reaction, sensation of chill and tendency to cluster, are similar to the symptoms of patients with KYDS. This method was going to be applied in this study.

A recent research had demonstrated that the levels of proinflammatory cytokines and chemokines (interleukin-6 (IL-6), monocyte chemoattractant protein-1 (MCP-1) and tumor necrosis factor-α (TNF-α)) significantly increased in viral pneumonia in mice with KYDS, which highlighted the fact that KYDS was closely bound up with the immune response[8]. Moreover, many studies published in Chinese language also revealed the relationship between KYDS and immune response[9,10]. It is well known that host innate immune system plays a critical role in triggering the release of aforementioned proinflammatory cytokines and chemokines. And the pivotal event is the recognition of foreign substances by pattern recognition receptors, including Toll-like receptors (TLRs), retinoic acid-inducible gene-I (RIG-I)-like receptors (RLRs) and nucleotide-binding

*Corresponding author

oligomerization domain (NOD)-like receptors (NLRs)[11]. Especially, RIG-I signaling pathway has received extensive attention in recent years[12-14].

Normally, RIG-I is held in an inactive, closed conformation. The activation starts upon recognizing and binding to viral RNA by RIG-I helicase and regulatory domains. After that, the caspase activator recruitment domains (CARDs) of RIG-I is ubiquitinated by tripartite motif containing 25 (TRIM25)[14]. Activated CARDs of RIG-I then interact with mitochondrial antiviral signaling adaptor MAVS/VISA/IPS-1/Cardif, thus giving rise to the activation of interferon regulatory factor 3 (IRF3) and nuclear factor κB (NF-κB) and inducing the production of Type I interferon and proinflamatory cytokines[15,16]. It had been demonstrated that RIG-I signaling pathway and its subsequent production of proinflammatory cytokines (TNF-α and IL-6) were involved in aging-related renal injury and inflammation in senescence-accelerated mice[17]. However, despite the fact that IL-6 and TNF-α were confirmed to be related to KYDS[8-10], no research has been done to investigate whether RIG-I-mediated innate immune response participates in the development of KYDS. More significantly, TLR4, the same pattern recognition receptor as RIG-I, has been confirmed to be related to KYDS in recent years[18,19]. Thus, trying to reveal the relationship between RIG-I and KYDS tends to be the purpose of this study.

YGP, a classic TCM formula, was first recorded in Jingyue Quanshu in the year 1624. Based on the function of warming up kidney yang, it has been used to treat patients of KYDS for about 400 years. Many studies showed that YGP had notable curative effectiveness for KYDS[1,18,20]. Moreover, it had been proved to have anti-inflammatory effects on host immune response in the treatment of osteoarthritis and experimental autoimmune encephalomyelitis[21-23]. For these two reasons, this study was designed to elucidate its potential effects exerting on RIG-I-mediated innate immune response in rats suffering from KYDS induced by hydrocortisone.

## Methodology

### Animals

Fifty-six male Wistar rats (Grade SPF, 7 weeks, 250±20 g) were purchased from Experimental Animal Center of Hubei Province (No. SCXK (E) 2015-0018, Wuhan, China). Rats were reared under standard laboratory conditions (temperature of 22±2℃, humidity of 55±10%, light/dark cycle of 12 h/12 h) with food and water freely available. All procedures involving laboratory animals were performed in accordance with the WHO International Guiding Principles for Biomedical Research Involving Animals and were approved by the local ethics committee of Hubei University of Chinese Medicine.

### Modeling and drug administration

Following acclimatization for 1 week, rats (8 weeks) were randomly divided into 4 groups: (a) normal healthy control rats (N, n=14); (b) KYDS model rats (M, n=14); (c) KYDS model rats with YGP (Henan Wanxi Pharmaceutical Co., Ltd., Nanyang, China) at the low dose of 2.43 g/kg/d, which is equivalent to the clinical dosage (YL, n=14); (d) KYDS model rats with YGP at the high dose of 4.86 g/kg/d (YH, n=14). KYDS model rats were induced by intramuscular injection of hydrocortisone (Lijun Pharmaceutical Co., Ltd., Xi'an, China) at the dose of 10 mg/kg/d for 15 days as previously described[7], while the rats in the normal group were treated with equal volume of physiological saline. After KYDS models established successfully, the above-mentioned concentrations of YGP were administered intragastrically to KYDS model rats at the volume of 10 mL/kg/d for 30 days in YL and YH groups, whereas rats in N and M groups were treated with equal amount of distilled water. Rats were visually inspected for health conditions and weighed every three days for adjusting the dosage.

### Weight measurement and spleen isolation

Body weight of all rats was measured and analyzed on the last day of 3 stages, including Stage I (8 weeks, after acclimatization of rats), Stage II (10 weeks, after establishment of KYDS models) and Stage III (14 weeks, after administration of YGP). Data were analyzed using SPSS 22.0 and values were presented as mean±standard deviation ($\bar{x}$±s). After administration of YGP, rats were decapitated under ether anesthesia and spleens were rapidly separated for gross appearance observation, spleen index measurement and further analysis. Spleen index is equal to spleen weight divided by body weight.

### Enzyme-linked immunosorbent assay (ELISA)

Urine was collected for 24 h from rats in each group and stored frozen at −20°C until ELISA assay on the last day of the 10th week and the last day of the 14th week. Then urinary 17-hydroxycorticosteroid (17-OHCS) was measured using an ELISA kit (Jiancheng Bioengineering Institute, Nanjing, China) in accordance with the manufacturer's instructions.

**Real-time quantitative reverse transcription polymerase chain reaction (qRT-PCR) assay**

Total RNA was isolated from spleens using a RNeasy Mini Kit (Qiagen, Valencia, CA, USA) and contaminating genomic DNA was removed by DNase I digestion (Takara, Kyoto, Japan). 1 μg purified RNA was reverse-transcribed to cDNA using a M-MLV RTase cDNA Synthesis Kit (Takara, Kyoto, Japan). qRT-PCR amplification was performed using iQTM SYBR® Green Supermix (Bio-Rad, Hercules, California, USA) with iQTM5 Multicolor Real-Time PCR Detection System (Bio-Rad, Hercules, California, USA). A typical amplification system consisted of 2 μL cDNA, 0.5 μL of 5' and 3' primers and 12.5 μLi QTM SYBR® Green Supermix, and it was adjusted to a final volume of 25 μL with distilled water. The amplification parameters were set as follows: 1 cycle of predenaturation for 2 min at 95℃ and 45 cycles of 5 s at 95℃, 15 s at 56℃ and 30 s at 72℃. Fluorescence data were acquired at the 72℃ step and during the melting-curve program. The primer sequences are shown in Table 1 and relative mRNA abundances are calculated according to $2^{-\Delta\Delta CT}$ method using β-Actin as the internal reference gene.

**Western blotting and immunoprecipitation analysis**

Spleen tissues were homogenized and treated with 200 μL of RIPA lysis buffer (Bi Yuntian, Hefei, China) for 30 min on ice. After centrifugation at 12000 g for 30 min at 4℃, the supernatants were collected and protein concentrations were quantitated via a bicinchoninic acid protein assay kit (Pierce, Rockford, Illinois, USA). For immunoblotting assay, equivalent amounts of protein samples were mixed with 4× laemmli buffer and boiled for 10 min and then separated by 10% SDS-polyacrylamide gel electrophoresis and transferred onto nitrocellulose membranes (GE Healthcare, Buckinghamshire, UK). The membranes were blocked with 5% nonfat milk and incubated with primary antibodies (anti-TRIM25 (1:1000, Ab203210, Abcam, Cambridge, UK), anti-TNFα (1:2000, Ab6671, Abcam, Cambridge, UK), anti-IL6 (1:2000, Ab9324, Abcam, Cambridge, UK), anti-β-Actin (1:5000, 66009-1-Ig, Protein Tech, Chicago, USA) over night at 4℃, followed by incubating with HRP-conjugated secondary antibodies (goat anti-mouse IgG, (1:5000, sc-2031, Santa Cruz Biotechnology Inc., Santa Cruz, California, USA) or goat anti-rabbit IgG (1:5000, sc-2030, Santa Cruz Biotechnology Inc., Santa Cruz, California, USA)) for 1 h on a rocker. Results were visualized using a chemiluminescence detection kit (Bi Yuntian, Hefei, China).

For immunoprecipitation assay, a fraction of whole cell lysate was used as the input and remain sample was incubated with 10 μL of 50% protein A/G-sepharose beads (Abmart, Shanghai, China) for 10 min. After centrifugation at 12000 g for 5 min at 4℃, the supernatants were collected and incubated with 2 μL anti-RIG-1 antibody (Ab45428, Abcam, Cambridge, UK) over night at 4℃, followed by incubating with 20 μL of 50% protein A/G-sepharose beads for 2 h at 4℃. After centrifugation at 1000 g for 5 min at 4℃, the beads were collected and washed by RIPA lysis buffer (Bi Yuntian, Hefei, China), and followed by eluting with 25 μL 4× laemmli buffer (Bi Yuntian, Hefei, China) and boiling for 10 min. After centrifugation at 12000 g for 10 min, the supernatants were collected and analyzed by western blotting assay using anti-Ubiquitin (1:1000, Ab7780, Abcam, Cambridge, UK) as primary antibody, while the input was analyzed simultaneously using anti-RIG-I (1:2000) or anti-β-Actin (1:5000) as primary antibody. Remaining steps referred to western blotting assay.

**Immunolohistochemistry analysis**

Spleen tissues were fixed in 4% paraformaldehyde for 24 h at 4℃ and subsequently embedded with paraffin. The paraffin sections of spleen were deparaffinized with xylene and rehydrated through a graded alcohol series. Antigen retrieval was performed using 0.01 M citrate buffer (pH 9.0) at 95℃ for 15 min, followed by quenching with 3% hydrogen peroxide. After treatment in 10% normal goat serum (Gibco, Carlsbad, California, USA) at room temperature for 30 min, the sections were incubated with the primary antibodies (anti-RIG-I (1:200), anti-TRIM25 (1:200), anti-TNFα (1:100) and anti-IL6 (1:200)) over night at 4℃. The sections were then rinsed in PBS and incubated with HRP-conjugated secondary antibodies and visualized with diaminobenzidine substrate (Maixin Biotechnology, Fuzhou, China). The slides were counterstained with hematoxylin and observed using a light microscope (BX53, Olympus, Tokyo, Japan).

Table 1 — Primers used in real-time PCR

| Gene | Forward primer (5' to 3') | Reverse primer (5' to 3') |
|---|---|---|
| β-Actin | CGTTGACATCCGTAAAGAC | TAGGAGCCAGGGCAGTA |
| RIG-I | AAGCGTGCTCAGTGTTT | ATTTCCGCAAATGTGAT |
| TRIM25 | CCGTCAAGGCTAAGGT | TGTGGGCGGTATTGTA |
| TNF-α | CACCACGCTCTTCTGTC | CTACGGGCTTGTCACTC |
| IL-6 | CTTCTTGGGACTGATGTT | ACTGGTCTGTTGTGGGT |

## Results

**Effect on body weight of rats**

As illustrated in Table 2, body weight of all rats showed no significant differences in Stage I ($^{a}p>0.05$). In Stage II, body weight of KYDS rats in group M, YL and YH decreased significantly compared with that of healthy control rats in group N ($^{b}p<0.001$, $^{c}p=0.001$). In Stage III, body weight of KYDS rats in group M reduced dramatically compared with that of healthy control rats in group N ($^{d}p<0.001$), while YGP administration reversed them towards normal level in a dose-dependent manner in group YL and YH compared with that of KYDS rats in group M ($^{e}p<0.001$).

**Effect on 17-OHCS in urine of rats**

ELISA results (Table 3) revealed that urinary 17-OHCS of KYDS rats in group M, YL and YH decreased significantly compared with that of healthy control rats in group N ($^{a}p<0.001$) in Stage II. In Stage III, urinary 17-OHCS of KYDS rats in group M reduced dramatically compared with that of healthy control rats in group N ($^{b}p<0.001$), while YGP administration reversed them towards normal level in a dose-dependent manner in group YL and YH compared with that of KYDS rats in group M ($^{c}p<0.01$).

**Effect on spleens of rats**

As the maximal immune organ, spleen plays a crucial role in immune reaction. On the basis of this fact, rat spleens were analyzed in this study. As shown in (Fig. 1A) the size of spleens in KYDS rats was obviously shrinked compared with that of healthy control rats, while YGP treatment relieved the degree of this shrinkage in a dose-dependent manner. Moreover, in (Fig. 1B) the spleen index in KYDS rats ($^{a}p<0.01$) was obviously reduced compared with that of healthy control rats, while the reduction was rescued by YGP treatment ($^{b}p<0.05$).

Table 2 — Effect on body weight of rats ($\bar{x} \pm s$, g)

| | Stage I (8 weeks) | Stage II (10 weeks) | Stage III (14 weeks) |
|---|---|---|---|
| N | 258.9±11.9 | 294.9±12.7 | 344.1±12.2 |
| M | 263.2±13.9[a] | 271.3±16.1[b] | 290.8±15.5[d] |
| YL | 260.4±14.1[a] | 268.5±15.8[b] | 314.6±13.2[e] |
| YH | 264.7±14.4[a] | 273.7±15.4[c] | 331.1±11.8[e] |

Stage I: 8 weeks, after acclimatization of rats; Stage II: 10 weeks, after establishment of KYDS models; Stage III: 14 weeks, after administration of YGP. N: the weight of normal healthy control rats; M: the weight of KYDS model rats induced by hydrocortisone; YL: the weight of KYDS model rats treated with YGP (2.43 g/kg/d); YH: the weight of KYDS model rats treated with YGP (4.86 g/kg/d). [a]P>0.05, compared with group N in Stage I; [b]P<0.001, [c]P = 0.001, compared with group N in Stage II; [d]P<0.001, compared with group N in Stage III; [e]P<0.001, compared with group M in Stage III.

Table 3 — Effect on 17-OHCS in urine of rats ($\bar{x} \pm s$, nmol/L)

| | StageII(10weeks) | StageIII (14weeks) |
|---|---|---|
| N | 11.401±1.249 | 12.184±0.299 |
| M | 6.196±0.225[a] | 6.641±0.203[b] |
| YL | 5.976±0.27[a] | 8.703±0.569[c] |
| YH | 6.357±0.212[a] | 9.167±0.717[c] |

Stage II: 10 weeks, after establishment of KYDS models; Stage III: 14 weeks, after administration of YGP. N: the level of urinary 17-OHCS in normal healthy control rats; M: the level of urinary 17-OHCS in KYDS model rats induced by hydrocortisone; YL: the level of urinary 17-OHCS in KYDS model rats treated with YGP (2.43 g/kg/d); YH: the level of urinary 17-OHCS in KYDS model rats treated with YGP (4.86 g/kg/d). [a]P<0.001, compared with group N in Stage II; [b]P< 0.001, compared with group N in Stage III; [c]P<0.01, compared with group M in Stage III.

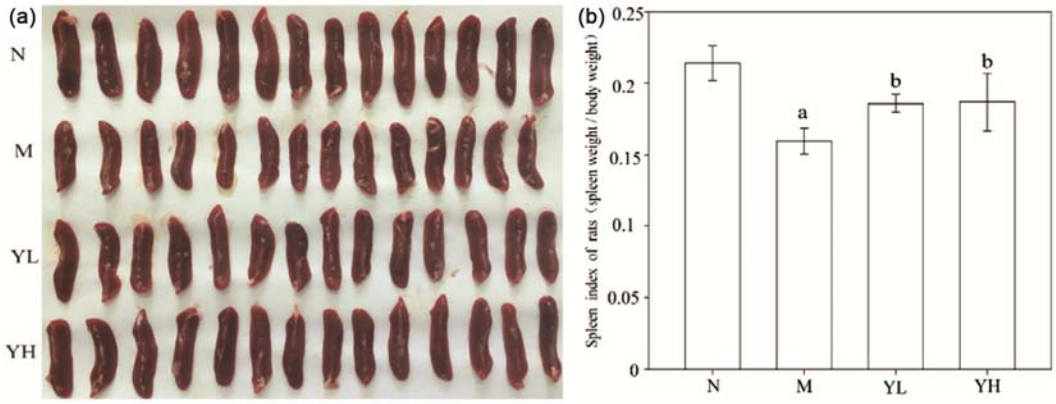


Fig. 1 — Effect on spleens of rats. (A): Morphological size of spleen. (B): Weight index of spleen. [a]P<0.01, compared with group N; [b]P<0.05, compared with group M. N: normal healthy control rats; M: KYDS model rats induced by hydrocortisone; YL: KYDS model rats treated with YGP (2.43 g/kg/d); YH: KYDS model rats treated with YGP (4.86 g/kg/d).

**Effect on expression, ubiquitination and distribution of RIG-I in spleens of rats**

RIG-I, activated by TRIM25-mediated ubiquitination, plays a crucial role in host innate immune system. A series of measures were applied to explore the expression, ubiquitination and distribution of RIG-I in rat spleens to study the effect of KYDS modeling and subsequent administration of YGP in rats.

Relative expression levels of RIG-I mRNA were determined using qRT-PCR assay. As (Fig. 2A) presents, the mRNA expression level dramatically increased in the spleens of KYDS rats ($^{a}p<0.001$) compared with that of healthy control rats. Following the administration of YGP, the remarkable increase was effectively reversed, tending to close to the normal level in a dose-dependent manner ($^{b}p<0.001$), compared with that in KYDS rats.

Furthermore, given that ubiquitination of N-terminal CARDs is vital for the activation of RIG-I to trigger subsequent immune responses, the assessment of endogenous RIG-I polyubiquitination level was conducted by combining western blotting with immunoprecipitation analysis. The results demonstrated that endogenous RIG-I polyubiquitination underwent markedly enhanced in the spleens of KYDS rats, compared with that of healthy control rats. Undoubtedly, this tendency was potently suppressed by the administration of YGP in a dose-dependent manner (Fig. 2B).

Finally, Results of immunohistochemistry staining (Fig. 2C & Fig. 2D) confirmed that the distribution of RIG-I protein exhibited the same tendency. In normal health rats, the spleen section showed scattered granular signals of brown staining and low percentage of positive cells. KYDS challenge caused significantly advanced staining intensity, giving rise to concentrated signal distribution of dark brown staining and higher percentage of positive cells ($^{a}p<0.001$). The additional administration of YGP effectively diminished the density of signals, reversing to the scattered distribution, with the staining intensity still stronger than the normal level. Also, the YGP treatment can lower the percentage of positive cells compared to KYDS challenge ($^{b}p<0.01$, $^{c}p<0.001$).

**Effect on expression and distribution of TRIM25 in spleens of rats**

TRIM25, an E3 ubiquitin ligase, is necessary for the activation of RIG-I through attachment of polyubiquitin chains, which plays a vital role in triggering innate immune response. Given that

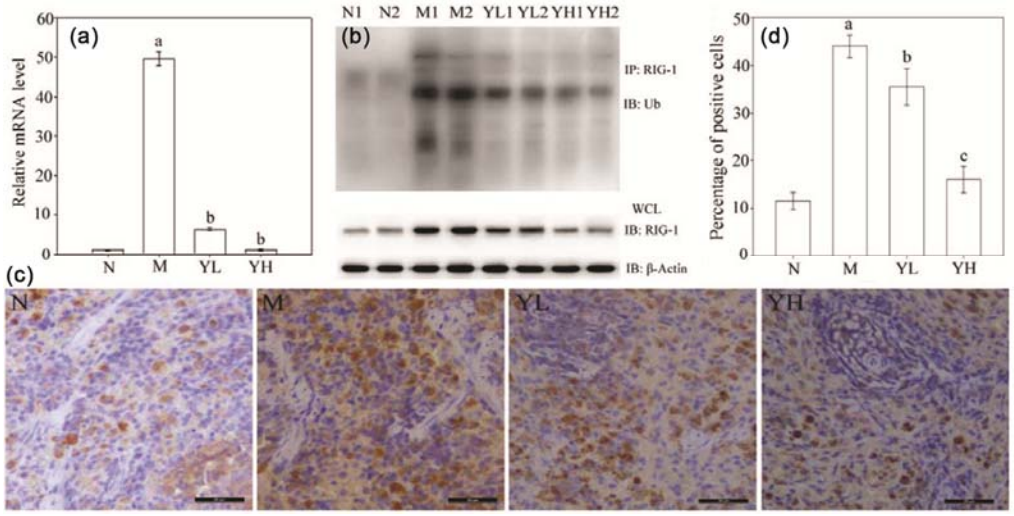


Fig. 2 — Effect on expression, ubiquitination and distribution of RIG-I in spleens of rats

(A): Relative mRNA levels of RIG-I. The mRNA levels of 14 rats in each group were determined using qRT-PCR assay by normalizing to β-Actin. Data indicate the mean ± standard deviation of three independent experiments. $^{a}P<0.001$, compared with group N; $^{b}P<0.001$, compared with group M. (B): Endogenous polyubiquitination of RIG-I. Endogenous polyubiquitination of RIG-I was analyzed by immunoprecipitation with anti-RIG-I and subsequent immunoblot with anti-Ubiquitin using WCL as the input and anti-β-Actin as the control. The protein sample of 7 rats in each group was analyzed as a whole. (C): Distribution of RIG-I. Immunohistochemistry staining was performed using anti-RIG-I (bar=20 μm). (D): Percentage of positive cells derived from the immunohistochemistry staining result. $^{a}P<0.001$, compared with group N; $^{b}P<0.01$, $^{c}P<0.001$, compared with group M. N: normal healthy control rats; M: KYDS model rats induced by hydrocortisone; YL: KYDS model rats treated with YGP (2.43 g/kg/d); YH: KYDS model rats treated with YGP (4.86 g/kg/d). RIG-I: retinoic acid-inducible gene-I; Ub: Ubiquitin; WCL: whole cell lysate.

endogenous polyubiquitination of RIG-I was affected by KYDS challenge and additional YGP administration, the effect on TRIM25 was explored.

qRT-PCR assay results (Fig. 3A) demonstrated that the mRNA expression of TRIM25 also increased in the spleens of KYDS rats ($^{a}p<0.001$), compared with that of healthy control rats, but the trend of increase was lower than that of RIG-I. Additional administration of YGP also reversed the increase caused by KYDS challenge in a dose-dependent manner ($^{b}p=0.001$, $^{c}p<0.001$), compared with that of KYDS rats.

Moreover, western blotting analysis (Fig. 3B) revealed that the expression level of TRIM25 protein was enhanced in the spleens of KYDS rats ($^{a}p<0.001$) compared with that in normal healthy control rats. However, this enhancement was suppressed by the subsequent administration of YGP in a dose-dependent manner ($^{b}p<0.01$, $^{c}p<0.001$).

Finally, immunohistochemistry staining results (Fig. 3C & Fig. 3D) confirmed that the distribution of TRIM25 protein exhibited very few scattered dot signals of weak light brown staining in the spleen section of normal health rat and low percentage of positive cells, whereas the staining intensity significantly enhanced in the spleen section of KYDS rat, resulting in dramatically higher percentage of positive cells ($^{a}p<0.001$). Besides, the additional administration of YGP gave rise to the moderate level of staining signals, which is stronger than the N group but weaker than the M group. Also, the YGP treatment can efficiently lower the percentage of positive cells compared to KYDS challenge ($^{b}p<0.001$).

**Effect on expression and distribution of TNF-α and IL-6 in spleens of rats**

After ubiquitination and activation by TRIM25, RIG-I is involved in the activation of interferon regulatory factor 3 and nuclear factor κB and the induction of type I interferon and proinflamatory cytokines. To further determine whether RIG-I is functional to respond to KYDS challenge and additional YGP administration, the expression and distribution of the critical downstream proinflammatory mediators (TNF-α and IL-6) were investigated.

qRT-PCR assay results (Fig. 4A) demonstrated that the mRNA expression levels of TNF-α and IL-6 were sharply increased in the spleens of KYDS rats, compared with that of healthy control rats ($^{a}p<0.001$,

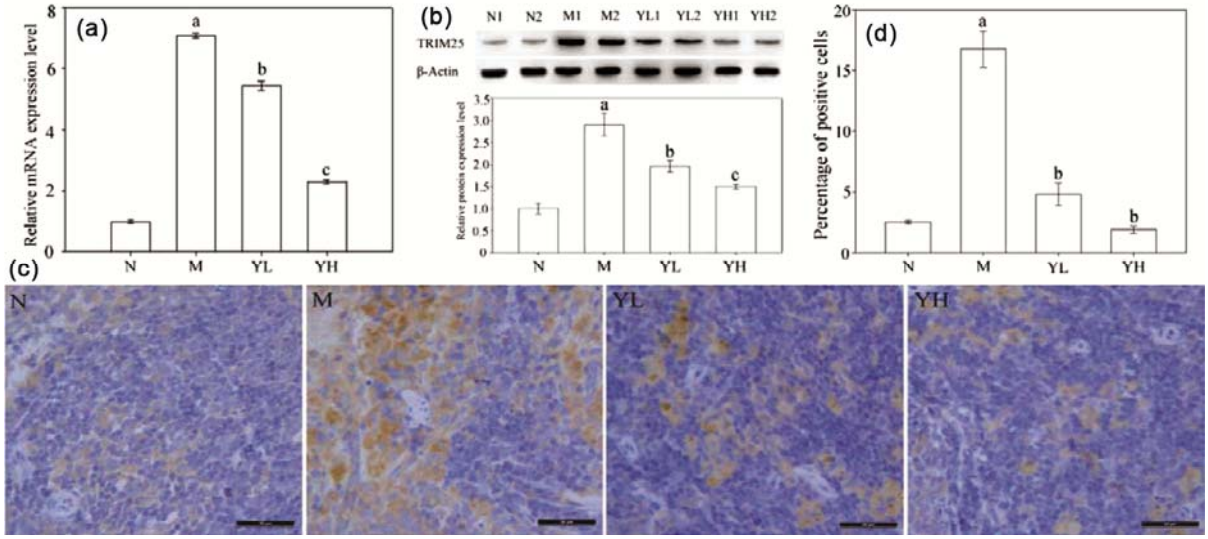


Fig. 3 — Effect on expression and distribution of TRIM25 in spleens of rats

(A): Relative mRNA levels of TRIM25. The mRNA levels of 14 rats in each group were determined using qRT-PCR assay by normalizing to β-Actin. Data indicate the mean ± standard deviation of three independent experiments. $^{a}p<0.001$, compared with group N; $^{b}P=0.001$, $^{c}P<0.001$, compared with group M. (B): Protein levels of TRIM25. Protein levels were determined by western blotting with anti-TRIM25, using anti-β-Actin as the control. The protein sample of 7 rats in each group was analyzed as a whole. Data of relative protein expression level indicate the mean ± standard deviation of three independent experiments. $^{a}p<0.001$, compared with group N; $^{b}p<0.01$, $^{c}p<0.001$, compared with group M. (C): Distribution of TRIM25. Immunohistochemistry staining was performed using anti-TRIM25 (bar=20 μm). (D): Percentage of positive cells derived from the immunohistochemistry staining. $^{a}p<0.001$, compared with group N; $^{b}p<0.001$, compared with group M. N: normal healthy control rats; M: KYDS model rats induced by hydrocortisone; YL: KYDS model rats treated with YGP (2.43 g/kg/d); YH: KYDS model rats treated with YGP (4.86 g/kg/d). TRIM25: tripartite motif containing 25.

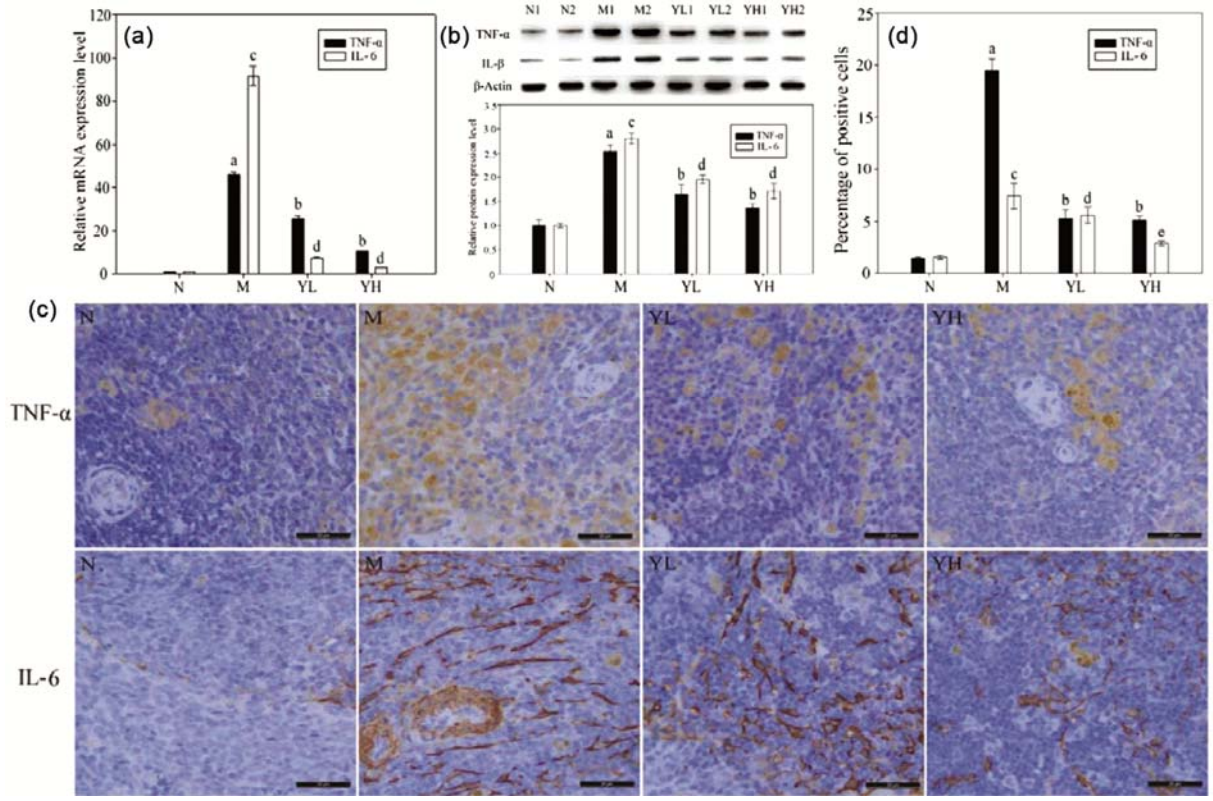


Fig. 4 — Effect on expression and distribution of TNF-α and IL-6 in spleens of rats

(A): Relative mRNA levels of TNF-α and IL-6. The mRNA levels of 14 rats in each group were determined using qRT-PCR assay by normalizing to β-Actin. Data indicate the mean ± standard deviation of three independent experiments. [a]p<0.001, [c]p<0.001, compared with group N; [b]p<0.001, [d]p<0.001, compared with group M. (B): Protein levels of TNF-α and IL-6. Protein levels were determined by western blotting with anti-TNF-α and anti-IL-6, using anti-β-Actin as the control. The protein sample of 7 rats in each group was analyzed as a whole. Data of relative protein expression level indicate the mean ± standard deviation of three independent experiments. [a]p<0.001, [c]p<0.001, compared with group N; [b]p<0.001, [d]p<0.001, compared with group M. (C): Distribution of TNF-α and IL-6. Immunohistochemistry staining was performed using anti-TNF-α and anti-IL-6 (bar=20 μm). D: Percentage of positive cells derived from the immunohistochemistry staining.[a]p<0.001, [c]p<0.001, compared with group N; [b]p<0.001, [d]p<0.05, [e]p<0.001, compared with group M. N: normal healthy control rats; M: KYDS model rats induced by hydrocortisone; YL: KYDS model rats treated with YGP (2.43 g/kg/d); YH: KYDS model rats treated with YGP (4.86 g/kg/d). TNF-α: tumor necrosis factor-α; IL-6: interleukin-6.

[c]p<0.001), among which the increasing trend of IL-6 was more significant. Subsequently, the two up-regulated expression levels induced by KYDS challenge were efficiently alleviated by YGP treatment in a dose-dependent manner ([b]p<0.001, [d]p<0.001).

Also, according to the analysis of western blot (Fig. 4B), the protein expression levels of TNF-α and IL-6 were evidently enhanced in the spleens of KYDS rats ([a]p<0.001, [c]p<0.001), compared with that of healthy control rats, whereas both the elevated expression levels were suppressed by YGP treatment in a dose-dependent manner ([b]p<0.001, [d]p<0.001).

Finally, the results of immunohistochemistry staining (Fig. 4C & Fig. 4D) provided more intuitive evidence for the variation of TNF-α and IL-6. In normal condition, the spleen sections exhibited very weak signals of these two factors and low percentage of positive cells. Responding to KYDS challenge, the staining intensity was dramatically enhanced, with the distribution of TNF-α showed concentrated dot signals, whereas the distribution of IL-6 exhibited stretched strip-like signals. Also, the percentage of positive cells was obviously increased ([a]p<0.001, [c]p<0.001) under the pressure of KYDS challenge. When it comes to YGP treatment, these two enhanced signal distribution patterns were effectively suppressed, leading to lower percentage of positive cells compared to KYDS challenge ([b]p<0.001, [d]p<0.05, [e]p<0.001).

## Discussion

In China, TCMs are widely used to prevent and treat a great number of diseases. When it comes to

immunological diseases, TCMs have performed well in clinical practices and played dual roles in the regulation of immune responses. It has been demonstrated that TCMs can not only exert stimulatory effects on immune cells, immune organs, cytokine production and tumorigenesis, but also exert inhibitory effects on inflammation, allergy, autoimmune disease and graft rejection[24-26]. Although many clinical practices have highlighted the immunomodulatory effects of TCMs, there is little experience and limited data to support this claim in animal models. As the establishment of KYDS model, it tends to be a good choice for revealing the role of TCMs in immune regulation. KYDS is applied in TCM to describe a state in which the patients show characteristic symptoms mainly including fatigue, thin stool, hearing impairment, soreness and weakness of waist and knees, looseness of teeth and cold feeling of whole body. Also, it is prevalent in immune-compromised patients and is closely bound up with the immune response[8-10]. Thus, our findings were in keeping with these previous studies and adopted hydrocortisone-treated rats as animal models to explore the immunomodulatory effects in the development of KYDS.

The essence of kidney in Chinese medicine includes the functions of hypothalamus-pituitary-adrenal cortex, thyroid and gonad. At present, the animal model of KYDS is mainly judged by whether it has the similar clinical manifestations to human KYDS and whether its thyroid, adrenal, reproductive capacity and immune level are disordered[27]. In this experiment, the pregnant rats in the model group had the symptoms of fatigue, weakness, reduced activity, weight loss, slowed reaction, sensation of chill and tendency to cluster. Moreover, the urinary 17-OHCS in the model rats is significantly decreased than that in the normal group. All these symptoms are similar to the symptoms of patients with KYDS and are consistent with previous studies, which give rise to the fact that our experimental model of kidney deficiency is successful.

YGP, a classic TCM formula, had been proved to have notable curative effectiveness for KYDS[1,18,20]. Undoubtedly, it was proved in this study. After hydrocortisone treatment, KYDS rats showed weight loss, fatigue, sluggish and tendency to cluster. YGP administration could make these manifestations improved. Moreover, YGP treatment effectively reversed the weight loss and spleen shrinkage in KYDS rats in a dose-dependent manner. Furthermore, YGP had been proved to have anti-inflammatory effect to regulate the host immune responses in previous study[21-23]. Thus, this study was designed to elucidate its potential effects exerting on immune responses in KYDS rats.

It has been demonstrated that levels of proinflammatory mediators (TNF-α and IL-6) significantly increased in animal models with KYDS[8-10]. And it has been well known that RIG-I signaling pathway plays a critical role in triggering the release of proinflammatory mediators (TNF-α and IL-6)[15-17]. Based on these two facts, this study was aimed at investigating whether the RIG-I-mediated innate immune response participates in the development of KYDS in rats and evaluating the effect of YGP on RIG-I-mediated innate immune response in KYDS rats.

The results collectively showed that KYDS challenge not only strikingly increased the mRNA and protein expression levels of RIG-I but also markedly enhanced the endogenous RIG-I polyubiquitination levels in rat spleens, which could trigger host innate immune system. Whereas, subsequent YGP treatment effectively reversed this tendency in a dose-dependent manner in the spleens of KYDS rats, suggesting that the administration of YGP could relieve the RIG-I-mediated innate immune response induced by KYDS.

Normally, RIG-I is held in an inactive, closed conformation. And TRIM25 is necessary for the activation of RIG-I through attachment of polyubiquitin chains, which plays a vital role in triggering the RIG-I-mediated innate immune response. Consistent with the effect on RIG-I, KYDS challenge also enhanced the mRNA and protein expression levels of its activator (TRIM25), whereas, subsequent YGP treatment effectively reversed this tendency in a dose-dependent manner in the spleens of KYDS rats. These results indicated that TRIM25, as a necessary factor for activation of RIG-I, might play an important role in the immune stress response induced by KYDS and YGP treatment.

After ubiquitination and activation by TRIM25, RIG-I is involved in the activation of IRF3 and NF-κB and the induction of Type I interferon and proinflamatory cytokines. In this study, KYDS challenge obviously increased the mRNA and protein expression levels of the critical downstream proinflammatory mediators (TNF-α and IL-6) in rat spleens, suggesting that the RIG-I signaling pathway is functional to respond to the challenge via triggering the release of the aforementioned two factors.

Especially, the increase in the expression of these two factors was consistent with previous results revealed in animal models with KYDS[8-10]. However, additional YGP treatment effectively reversed the increase of these two factors in a dose-dependent manner in the spleens of KYDS rats, giving rise to a strong inference that the RIG-I-mediated innate immune response in KYDS rats was efficiently eased by YGP administration.

## Conclusion

The evidence presented in this study has revealed, for the first time, the levels of RIG-I, its activator (TRIM25) and its subsequent production (TNF-α and IL-6) all increased in the spleens of KYDS rats, demonstrating that RIG-I-mediated innate immune response was closely bound up with the development of KYDS. YGP at concentrations of 2.43 g/kg/d and 4.86 g/kg/d exhibited certain therapeutic effects on KYDS rats, via decreasing the levels of aforementioned factors in a dose-dependent manner in the spleens of KYDS rats. The fact that YGP can effectively regulate the host immune response in KYDS rats proposes a promising future for TCMs in immunomodulatory therapies.

## Conflicts of interests

The authors declare that there is no conflict of interest in connection with the work submitted.

## Acknowledgments

The authors thank the Scientific Research Projects of Hubei Provincial Department of Education (no. Q20152007) for financial support. The special thanks go to Prof Anfang Zhou and Prof. Jigang Cao, at School of Basic Medical Sciences, Hubei University of Chinese Medicine for giving advice on the experiments.

## References

1 Chen RQ, Wang J, Liao CB, Zhang L, Guo Q, *et al*., Exploring the biomarkers and therapeutic mechanism of Kidney-Yang deficiency syndrome treated by You-gui pill using systems pharmacology and serum metabonomics, *Rsc Advances*, 8 (2) (2018) 1098-1115.

2 Zheng P, Wang Y, Lu HM, Zhou XY, Tang T, *et al*., Plasma metabolomics analysis based on GC-MS in infertile males with Kidney-Yang deficiency syndrome, *Evid Based Complement Alternat Med*, 2017 (6) (2017) 1-11.

3 Yang S, Xu XF, Xu HF, Xu SY, Lin QH, *et al*., Purification, characterization and biological effect of reversing the Kidney-Yang deficiency of polysaccharides from semen cuscutae, *Carbohydrate Polymers*, 175 (2017) 249-256.

4 Chen RQ, Wang J, Liao CB, Ma N, Zhang L, *et al*., $^{1}$H NMR studies on serum metabonomic changes over time in a Kidney-Yang deficiency syndrome model, *Rsc Advances*, 7 (54) (2017) 34251-34261.

5 Lu XM, Xiong ZL, Li JJ, Zheng SN, Huo TG, *et al*., Metabonomic study on 'Kidney-Yang deficiency syndrome' and intervention effects of Rhizoma Drynariae extracts in rats using ultra performance liquid chromatography coupled with mass spectrometry, *Talanta*, 83 (3) (2011) 700-708.

6 Wang CM, Xu SY, Lai S, Geng D, Huang JM, *et al*., Curculigoorchioides (Xian Mao) modifies the activity and protein expression of CYP3A in normal and Kidney-Yang deficiency model rats, *Journal of Ethnopharmacology*, 144 (1) (2012) 33-38.

7 Tan Y, Liu XR, Lu C, He XJ, Li J, *et al*., Metabolic profiling reveals therapeutic biomarkers of processed Aconitum Carmichaeli Debx in treating hydrocortisone induced Kidney-Yang deficiency syndrome rats, *Journal of Ethnopharmacology*, 152 (3) (2014) 585-593.

8 Rong R, Li RR, Hou YB, Li J, Ding JX, *et al*., Mahuang-Xixin-Fuzi decoction reduces the infection of influenza A virus in Kidney-Yang deficiency syndrome mice, *Journal of Ethnopharmacology*, 192 (2016) 217-224.

9 Ji PZ, Zhang Y, Li XP, Zhang YX, Jian SN, *et al*., Effect of Fuzi Lizhong Tang on expression of NF-κB, TNF-α, IL-1β of Spleen and Kidney Yang deficiency type ulcerative colitis rats through enema, *Chinese Journal of Experimental Traditional Medical Formulae*, 21 (14) (2015) 124-128. (in Chinese)

10 Wu F, Zhang HM, Chen XG, Wang YP, Dong CW, *et al*., Change of glucocorticoid receptor, IL-1β and tumor TNF-α in rats with chronic renal failure of Kidney-Yang deficiency, *Journal of Emergency in Traditional Chinese Medicine*, 22 (4) (2013) 560-562. (in Chinese)

11 Vajjhala PR, Ve T, Bentham A, Stacey KJ & Kobe B, The molecular mechanisms of signaling by cooperative assembly formation in innate immunity pathways, *Molecular Immunology*, 86 (2017) 23-37.

12 Lee J, Park EB, Min J, Sung SE, Jang Y, *et al*., Systematic editing of synthetic RIG-I ligands to produce effective antiviral and anti-tumor RNA immunotherapies, *Nucleic Acids Research*, 46 (4) (2018) 1635-1647.

13 Sun XN, Feng WJ, Guo YD, Wang Q, Dong CY, *et al*., MCPIP1 attenuates the innate immune response to influenza A viruse by suppressing RIG-I expression in lung epithelial cells, *Journal of Medical Virology*, 90 (2) (2018) 204-211.

14 Hu Y, Li W, Gao T, Cui Y, Jin YW, *et al*., The severe acute respiratory syndrome coronavirus nucleocapsid inhibits type I interferon production by interfering with TRIM25-mediated RIG-I ubiquitination, *Journal of Virology*, 91 (8) (2017) e02143-16.

15 Li L, Yang RL, Feng MJ, Guo YC, Wang YX, *et al*., RIG-I is involved in inflammation through the IPS-1/TRAF$^{6}$, pathway in astrocytes under chemical hypoxia, *Neuroscience Letters*, 672 (2018) 46-52.

16 Kouwaki T, Okamoto M, Tsukamoto H, Fukushima Y, Matsumoto M, *et al*., Zyxin stabilizes RIG-I and MAVS interactions and promotes Type I interferon response, *Scientific Reports*, 7 (1) (2017) 11905-11917.

17 Zeng Y, Wang PH, Zhang M & Du JR, Aging-related renal injury and inflammation are associated with downregulation of Klotho and induction of RIG-I/NF-κB signaling pathway in senescence-accelerated mice, *Aging Clinical & Experimental Research*, 28 (1) (2016) 69-76.

18 Tan CE, Feng WZ, Chen JY & Yang F, Effect of Yougui Pills on TLR4/MyD88/NF-κB signal pathway of patients with Kidney-Yang deficiency syndrome, *Modern Journal of Integrated Traditional Chinese and Western Medicine*, 25(14) (2016) 1483-1485. (in Chinese)

19 Zhang Y, Hu XY & Yang F, Effect of Wenshen Prescription on TLR4/IL-6 signaling pathway in chronic hepatitis B patients with high ALT Level and Kidney Yang deficiency syndrome, *Chinese Journal of Experimental Traditional Medical Formulae*, 24(11) (2018) 150-155. (in Chinese)

20 Li WX, Zhang KQ, Liu Z, Liu L, Cheng Y, *et al*., Effect of Zuogui pill and Yougui pill on osteoporosis: a randomized controlled trial, *Journal of Traditional Chinese Medicine*, 38 (1) (2018) 33-42.

21 Zhang L, Wang PE, Ying J, Jin X, Luo C, *et al*., Yougui pills attenuate cartilage degeneration via activation of TGF-β/Smad signaling in chondrocyte of osteoarthritic mouse model, *Frontiers in Pharmacology*, 8 (2017) 611-621.

22 Wang YZ, Kou S, Gu LY, Zheng Q, Li M, *et al*., Effects of Zuogui pill, and Yougui pill on the expression of brain-derived neurotrophic factor and cyclic adenosine monophosphate/protein kinase A signaling transduction pathways of axonal regeneration in model rats with experimental autoimmune encephalomyelitis, *Chinese Journal of Integrative Medicine*, 20 (1) (2014) 24-30.

23 Ji XM, Liu HL, An C, Wang YQ, Zhao H, *et al*., You-Gui pills promote nerve regeneration by regulating netrin1, DCC and Rho family GT Pases Rho A, Racl, Cdc42 in C57BL/6 mice with experimental autoimmune encephalomyelitis, *Journal of Ethnopharmacology*, 187 (2016) 123-133.

24 Ren Y, Qiao W, Fu DL, Han ZW, Liu W, *et al*., Traditional Chinese Medicine protects against cytokine production as the potential immunosuppressive agents in atherosclerosis, *Journal of Immunology Research*, 2017 (10) (2017) 7424307-7424314.

25 Ma HD, Deng YR, Tian ZG & Lian ZX, Traditional Chinese Medicine and immune regulation, *Clinical Reviews in Allergy & Immunology*, 44 (3) (2013) 229-241.

26 Meng MB, Wen QL, Cui YL, She B & Zhang RM, Meta-analysis: Traditional Chinese Medicine for improving immune response in patients with unresectable hepatocellular carcinoma after trans catheter arterial chemoembolization, *Explore the Journal of Science & Healing*, 7 (1) (2011) 37-43.

27 Li JJ, Zhou Y, Li ZH & Xu XY, Improvement of Yougui Decoction on rats with adenine-induced kidney deficiency and immunodeficiency, *China Journal of Traditional Chinese Medicine and Pharmacy*, 34 (4) (2019) 1436-1439. (in Chinese)